

Chemical Shifts in Silatrane and Its Derivatives: A Study of the Transannular Interaction

Joseph H. Iwamiya[†] and Gary E. Maciel*

Contribution from the Department of Chemistry, Colorado State University, Fort Collins, Colorado 80523-0002

Received October 5, 1992

Abstract: Solid-state ^{13}C , ^{15}N , and ^{29}Si NMR spectra were obtained on silatrane and a series of derivatives. The isotropic ^{13}C chemical shifts are largely insensitive to substituent-induced structural changes. In contrast, the isotropic ^{15}N and ^{29}Si chemical shifts and chemical shift powder patterns are quite sensitive to substituent-induced structural changes. As the silicon-nitrogen internuclear distance ($r_{\text{Si-N}}$) decreases, the isotropic ^{15}N chemical shift increases and the isotropic ^{29}Si chemical shift decreases. The magnitude of the ^{15}N chemical shift anisotropy (CSA) decreases and the ^{29}Si CSA increases as $r_{\text{Si-N}}$ decreases. The change in δ_{\perp} and the CSA for ^{15}N is primarily due to the change in δ_{\perp} , which increases as $r_{\text{Si-N}}$ decreases. For ^{29}Si , all three principal elements change as $r_{\text{Si-N}}$ is varied. Variations in the ^{15}N chemical shift tensor elements are ascribed to changes in the N...Si transannular interaction. For the ^{29}Si chemical shift tensor, the observed changes are ascribed to a combination of effects due to changes in the transannular interaction and direct substituent effects. A simple molecular orbital treatment is useful in understanding the relationship between the transannular effect and the ^{15}N chemical shift tensor and in supporting the use of the ^{15}N chemical shift as an indicator of the transannular interaction.

Introduction

General Background. The isotropic chemical shift is an immensely useful parameter in the determination of chemical structure. This usefulness is largely due to empirical structure/chemical shift correlations. Because of the underlying, fundamental relationship between the chemical shift and electronic structure, serious efforts have been made to uncover correlations with electronic structure and reactivity parameters, e.g., electronegativity, inductive effects, etc.¹⁻⁹ Initially, these efforts were directed toward the isotropic chemical shifts of ^1H , ^{19}F , and ^{13}C , with other nuclides¹⁰⁻¹⁵ such as ^{31}P and ^{29}Si receiving attention more recently.

The isotropic chemical shift is the *average* value of the diagonal elements of the chemical shift tensor. Advances in solid-state NMR allow one to determine the orientation dependence, or anisotropy, of the chemical shift interaction.¹⁶⁻¹⁹ It is now possible to determine the principal elements of a chemical shift powder

pattern conveniently and the orientation of the principal axes with more effort. Hence, instead of settling for just the average value of the chemical shift powder pattern, one can now aim for values of the three principal elements and the corresponding orientations in a molecular axis system.

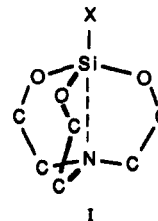
A priori, it seems likely, then, that when one attempts to correlate the chemical shift interaction with some structure or reactivity parameter, it should be more satisfactory, both fundamentally and empirically, if the correlation is established with the individual elements of the chemical shift tensor rather than the average. Such correlations have been presented recently for the chemical shift powder patterns of ^{31}P in phosphates,¹¹ ^{29}Si in zeolites,¹³ and ^{15}N in substituted benzonitriles;²⁰ these correlations typically involve a principal element or a combination of principal elements and a structural parameter, e.g., a bond length, bond angle, or a reactivity parameter.

In the work described here, the chemical shift parameters of the ^{13}C , ^{15}N , and ^{29}Si resonances in a set of 2,8,9-trioxa-5-aza-1-silabicyclo[3.3.3]undecanes (silatranes I, hydrogens not shown for simplicity) were determined from powdered, crystalline

* To whom correspondence should be addressed.

[†] Present address: Lockheed Missiles and Space, Palo Alto Research Laboratories, 3251 Hanover St., Palo Alto, CA 94304-1191.

- (1) Shoolery, J. N. *J. Chem. Phys.* **1953**, *21*, 1899.
- (2) Meyer, L. H.; Gutowsky, H. S. *J. Am. Chem. Soc.* **1953**, *75*, 481.
- (3) Spiess, H.; Schneider, W. G. *J. Chem. Phys.* **1961**, *35*, 772.
- (4) Gutowsky, H. S.; Hoffman, C. J. *J. Chem. Phys.* **1951**, *19*, 1259.
- (5) Taft, R. W. *J. Am. Chem. Soc.* **1957**, *79*, 1045.
- (6) Maciel, G. E.; Natterstad, J. J. *J. Chem. Phys.* **1965**, *42*, 2427.
- (7) Lauterbur, P. C. *J. Am. Chem. Soc.* **1961**, *83*, 1846.
- (8) Maciel, G. E. In *Topics in Carbon-13 NMR Spectroscopy*; Levy, G. E., Ed.; Wiley: New York, 1974; Vol. 1, p 54.
- (9) Savitsky, G. B.; Namikawa, K. *J. Phys. Chem.* **1964**, *68*, 1956.
- (10) Grimmer, A.-R. *Spectrochim. Acta* **1978**, *34A*, 941.
- (11) Turner, G. L.; Smith, K. A.; Kirkpatrick, R. J.; Oldfield, E. *J. Magn. Reson.* **1986**, *70*, 408.
- (12) Cheetham, A. K.; Clayden, N. J.; Dobson, C. M.; Jakeman, R. J. *J. Chem. Soc., Chem. Commun.* **1986**, 195.
- (13) Klinowski, J. *Prog. Nucl. Magn. Reson. Spectrosc.* **1984**, *16*, 237.
- (14) Grimmer, A.-R. *Chem. Phys. Lett.* **1985**, *119*, 416.
- (15) Janes, N.; Oldfield, E. *J. Am. Chem. Soc.* **1985**, *107*, 6769.
- (16) Haeberlen, U. *High Resolution NMR in Solids. Selective Averaging*; Academic Press: New York, 1976.
- (17) Mehring, M. *Principles of High Resolution NMR in Solids*, 2nd ed.; Springer-Verlag: Berlin-Heidelberg, 1983.
- (18) Fyfe, C. A. *Solid State NMR for Chemists*; CFC Press: Guelph, 1983.
- (19) Ernst, R. R.; Bodenhausen, G.; Wokaun, A. *Principles of Nuclear Magnetic Resonance in One and Two Dimensions*; Oxford University Press: Oxford, 1987.



samples, with and without magic-angle spinning. The various chemical shift parameters are discussed in terms of their relationships with known structure and reactivity parameters. A number of chemical shift parameters are presented that can be correlated with a known structural parameter, e.g., bond length. In addition, a qualitative discussion on the origins of the observed variations in the ^{15}N and ^{29}Si chemical shift powder patterns is presented.

Silatranes. Silatranes are a class of organosilicon compounds that feature a silicon atom that can be discussed as nominally

(20) Sardashti, M.; Maciel, G. E. *J. Phys. Chem.* **1988**, *92*, 4620.

pentacoordinate. The interest in silatranes is due to their intriguing molecular structure, biological activity, and patterns of chemical reactivity.²¹⁻²³ The most intriguing aspect of this structure is the existence of and influence of a "transannular bond" between the silicon and nitrogen atoms, as indicated by the dashed line drawn between the silicon and nitrogen atoms in structure I.

The fact that this transannular bond could exist in silatranes was demonstrated by Turley and Boer via a single-crystal X-ray study.²⁵ Other studies on silatranes have shown that the length of this transannular bond is dependent upon the substituent bound to the silicon atom, structural modifications on the silatrane framework, and the physical environment of the molecule, e.g., solid, liquid, gaseous, or solution.²²⁻²⁴ The silicon-nitrogen internuclear distance ($r_{\text{Si-N}}$) has been found to range from 2.02 Å for the chloro derivative (X = Cl) to 2.89 Å for the *trans*-dimethylphenylphosphine platinum derivative, with typical distances ranging up to 2.22 Å for the ethyl derivative.²³ These distances are considerably shorter than the sum of the van der Waals radii of 3.5 Å for silicon and nitrogen, yet the distances are longer than a conventional silicon-nitrogen covalent bond length of 1.7–1.8 Å found in tetracoordinate silicon compounds.²⁵ Hence, this transannular bond is not like a "normal" silicon-nitrogen bond, and one can consider this bond to be a very weak one.²² And as will be demonstrated later, the ¹⁵N and ²⁹Si chemical shift powder patterns are susceptible to substituent-induced changes in the length of this transannular bond.

Experimental Section

The chemicals used in synthesizing silatrane and a set of derivatives were used as obtained from the vendors without further purification. *N*-Chlorosuccinimide, concentrated aqueous hydrogen fluoride, and triethanolamine were obtained from the Aldrich Chemical Co. Tetramethoxysilane, triethoxysilane, and tetraethoxysilane were obtained from Petrarch Systems, Inc.

The chloro and fluoro derivatives, as well as the parent silatrane, were synthesized via the procedures reported by Frye et al.²⁶ The ethoxy and methoxy derivatives were synthesized via the procedure used by Samour.²⁷ The synthetic preparations were carried out under an inert N₂ atmosphere. For the fluorosilatrane synthesis, the reaction was performed in a polyethylene bottle under an Ar(g) atmosphere. The vinyl, phenyl, methyl, and chloropropyl derivatives were supplied by Prof. L. Sommer (University of California, Davis). The chloromethyl and ethyl derivatives were obtained from Petrarch Systems, Inc. The authenticity and purity of the silatrane derivatives were verified by the liquid-state 270-MHz ¹H NMR spectra.

¹³C CP/MAS spectra were obtained under one of two circumstances: (a) at 25.3 MHz on a home-built spectrometer or (b) at 50.3 MHz on a lab-modified Nicolet NT-200 spectrometer, employing a home-built CP/MAS probe with a stator/spinner assembly similar to that described by Gay.²⁸ A variable contact time experiment¹⁷ (performed on phenylsilatrane) indicated that the optimal ¹³C signal-to-noise ratio was obtained with a contact time of 1 ms. The recycle times ranged from 1 to 8 s, depending on the apparent T_{1H} behavior. The magic-angle spinning speed was 2.5 KHz. All ¹³C chemical shifts were referenced to the aromatic resonance in hexamethylbenzene, which has a chemical shift of 132.2 ppm with respect to TMS, and are reported here relative to TMS.

Natural-abundance ¹⁵N spectra were obtained under cross-polarization conditions, with and without magic-angle spinning: (a) at 20.3 MHz on the lab-modified Nicolet NT-200 spectrometer or (b) at 26.4 MHz on a lab-modified Chemagnetics M-260 spectrometer, employing a home-

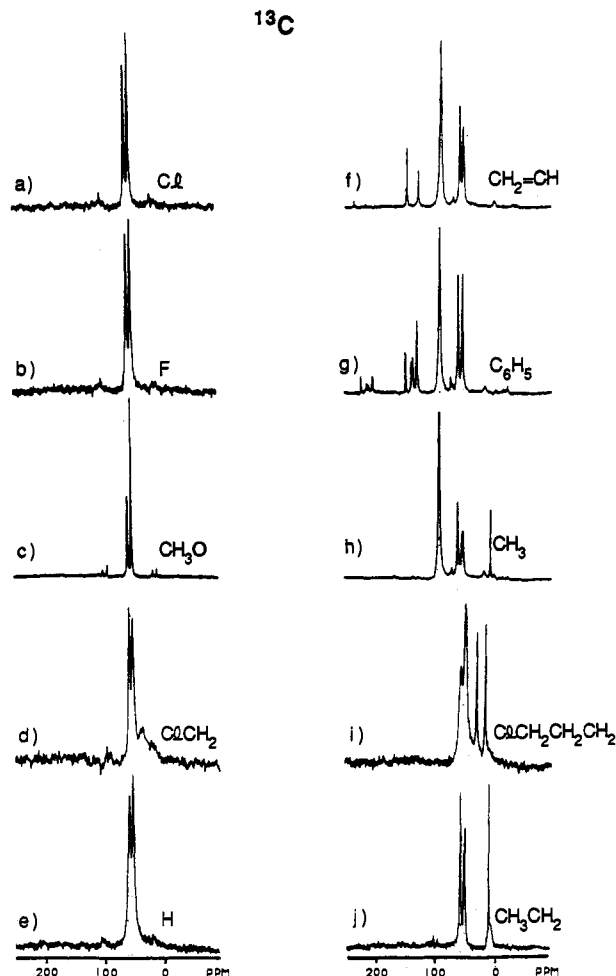


Figure 1. ¹³C CP/MAS spectra (50.3 MHz) of X-substituted silatranes, with X indicated. The peaks at 100 ppm in spectra f, g, and h are due to Delrin.

built CP/MAS probe with a stator/spinner assembly of the Delft design.²⁹ The optimal contact time (determined on methylsilatrane) was found to be 3 ms, with a recycle time ranging from 1 to 8 s, depending on apparent T_{1H} behavior. The magic-angle spinning speed was 3 kHz. All ¹⁵N chemical shifts were referenced to the ¹⁵N resonance of glycine, which has a chemical shift of 32.4 ppm with respect to liquid NH₃, and are reported here with respect to NH₃(l).

All ²⁹Si NMR spectra were obtained under cross-polarization conditions, with and without magic-angle spinning, at a ²⁹Si frequency of 39.8 MHz on the lab-modified Nicolet NT-200 spectrometer, employing a home-built CP/MAS probe using the stator/spinner assembly similar to the one described by Gay.²⁸ The optimal signal-to-noise ratio (determined on methoxysilatrane) was obtained with a contact time of 3 ms. The magic-angle spinning speed was 2.5 kHz. Tetrakis(trimethylsilyl)methane served as the ²⁹Si chemical shift reference. It has a chemical shift of -1.5 ppm with respect to TMS. ²⁹Si chemical shifts are reported here with respect to TMS.

The chemical shift convention used here is the δ scale, in which algebraically larger numbers indicate shifts to lower shielding. The symbol δ is used to label the chemical shift, and the convention, $\delta_{33} > \delta_{22} > \delta_{11}$, is employed for convenience.

Results and Discussion

¹³C Chemical Shifts. The ¹³C CP/MAS spectra of the silatranes examined here are shown in Figure 1, and the isotropic ¹³C chemical shifts are tabulated in Table I. Typically, the OCH₂ carbons of the silatrane framework have isotropic chemical shifts in the neighborhood of 58 ppm and the NCH₂ carbons have isotropic chemical shifts of approximately 51 ppm, as shown in Figure 2, which gives plots of these chemical shifts vs the Si-N

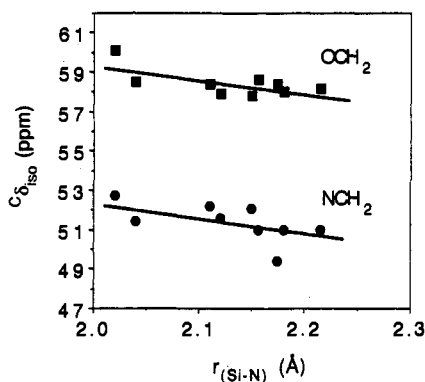
(29) Wind, R. A.; Antonio, F. E.; Duijvestijn, M. J.; Smidt, J.; Trommel, J.; deVette, G. M. C. *J. Magn. Reson.* 1983, 52, 424.

(21) Voronkov, M. G. *Pure Appl. Chem.* 1966, 13, 35.
 (22) Voronkov, M. G.; Dyakov, V. M.; Kirpichenko, S. V. *J. Organomet. Chem.* 1982, 233, 1.
 (23) Hencsei, P.; Parkanyi, L. *Rev. Silicon, Germanium, Tin Lead Compd.* 1985, 8, 191.
 (24) Shen, Q.; Hilderbrandt, R. L. *J. Mol. Struct.* 1980, 64, 257.
 (25) Turley, J. W.; Boer, F. P. *J. Am. Chem. Soc.* 1968, 90, 4026.
 (26) Frye, C. L.; Vincent, G. A.; Finzel, W. A. *J. Am. Chem. Soc.* 1971, 93, 6805.
 (27) Samour, C. M. U.S. Patent 3,118,921, 1964.
 (28) Gay, I. D. *J. Magn. Reson.* 1984, 58, 413.

Table I. Isotropic ^{13}C Chemical Shifts of Selected Silatranes in the Solid State^a

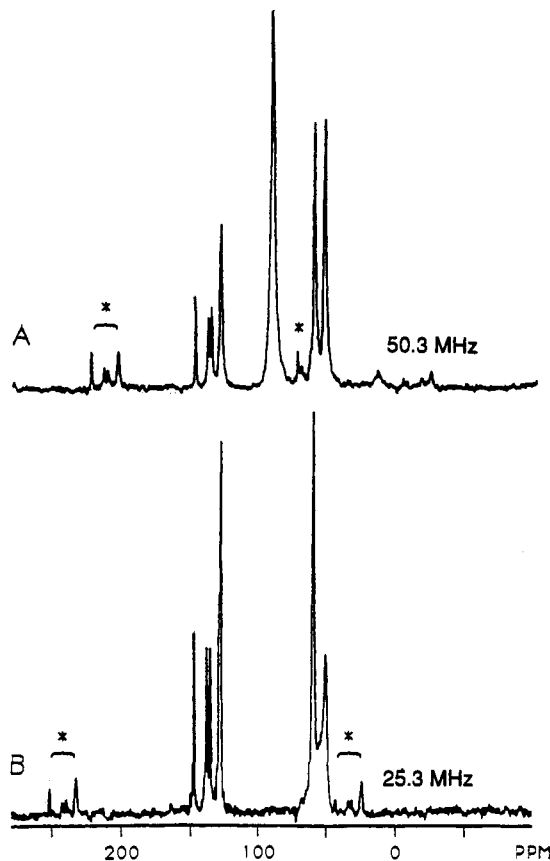
X	OCH ₂	NCH ₂	α	β	γ	δ
Cl	60.1	52.7				
F	58.5	51.4				
CH ₃ O	58.4	52.2		51.4		
ClCH ₂	57.9	51.6	35.0 ^b			
H	58.2	51.8				
CH ₂ CH	57.8	52.1	145.9	126.9		
				137.4 ^c		
C ₆ H ₅	58.6	51.0	146.8	134.6	127.1	128.1
		50.4 ^d				
CH ₃	58.4	49.2	3.8			
ClCH ₂ CH ₂ CH ₂	58.0	51.0 ^e	17.0	31.1	51.0 ^e	
CH ₃ CH ₂	58.2	51.0	11.0 ^e	11.0 ^e		

^a Obtained from ^{13}C CP/MAS spectra at 50.2 MHz. (α , β , γ , δ refer to positions in the substituent, relative to the Si atom.) Given in ppm relative to TMS(l). ^b Broad peak due to unaveraged ^{13}C -X dipolar couplings. X is ^{35}Cl or ^{37}Cl . ^c Splitting apparently due to conformational effects associated with the orientation of the phenyl ring with respect to the silatrane framework.²⁵ ^d Splitting apparently due to crystallographic disorder in the sample.^{21,22} ^e Spectral overlap between two resonances.

**Figure 2.** Correlation curves for the isotropic ^{13}C chemical shifts for the OCH₂ and NCH₂ vs $r_{\text{Si-N}}$. The lines are drawn for the viewers' eye.

distance. These assignments and the peak assignments for the substituents bound to the silicon atom are based upon solution-state ^{13}C NMR studies³⁰ and variable-field high-resolution solid-state ^{13}C NMR results. The variable-field studies, an example of which is shown in Figure 3 for phenylsilatrane, demonstrate the effect of the residual ^{13}C - ^{14}N heteronuclear dipole-dipole coupling,³¹ which becomes apparent as a broadening of the 51-ppm peak at the lower magnetic field (Figure 3B). In the high-resolution solid-state ^{13}C NMR spectrum of phenylsilatrane, the peaks in the 125–150-ppm range are assigned to the carbon nuclei of the benzene ring. The spinning sidebands due to these resonances are marked by asterisks in Figure 3. The peak at approximately 100 ppm in the spectrum in Figure 3A is due to the Delrin spinner. The lower-field broadening of the peak at 51 ppm identifies it as the NCH₂ carbons located in the silatrane rings.³¹

As with previously reported solution-state ^{13}C NMR studies,^{30,32} the isotropic ^{13}C chemical shift of silatranes in the solid state appears to be nearly independent of the Si-N distance, as seen in Figure 2. There does not appear to be an easily discernible or significant trend between the isotropic ^{13}C chemical shift and what one expects to be the most relevant geometric parameter, i.e., $r_{\text{Si-N}}$, the silicon-nitrogen internuclear distance. This perceived independence could be misleading in that *a priori* it is possible that *individual principal elements* of the ^{13}C chemical shift powder pattern might change in *opposite* directions, resulting in an isotropic chemical shift that gives the appearance of being

**Figure 3.** Effect of B_0 on ^{13}C CP/MAS spectra of phenylsilatrane. Spectra were collected at (A) 50.3 and (B) 25.3 MHz. Asterisks indicate spinning sidebands. The peak at 100 ppm in spectrum A is due to the Delrin spinner.

independent of substituent. A simple example would be the case of a chemical shift powder pattern in which the δ_{33} element increases by the same amount that the δ_{11} element decreases, with the δ_{22} element remaining constant; in this simplistic case, changes in two tensor elements cancel one another and the isotropic chemical shift remains the same. It is also possible *a priori* that the direct (electronic) effect of substituent variation on the isotropic ^{13}C chemical shifts of the silatrane ring carbons is small and its contribution to the isotropic ^{13}C chemical shifts could easily be masked by other local effects, e.g., neighbor anisotropy effects,³ slight changes in the bond lengths and bond angles, and solid-state intermolecular effects.⁸ In any case, the principal elements of the ^{13}C chemical shift tensors of substituted silatranes were not determined in this study because the techniques that would be required for overcoming peak overlaps in the static-sample powder patterns did not seem warranted in view of the anticipated complexity of interpretation of the ^{13}C tensor elements that would be obtained.

^{15}N Chemical Shifts. In contrast to the isotropic ^{13}C chemical shift, the isotropic ^{15}N chemical shift demonstrates a very clear correlation with $r_{\text{Si-N}}$. The principal elements of the ^{15}N chemical shift powder patterns, as well as the isotropic ^{15}N chemical shifts, are given in Table II. These values were derived from the ^{15}N chemical shift powder patterns of the various silatrane derivatives shown in Figure 4. The ^{15}N chemical shift powder patterns have shapes characteristic of axially symmetric tensors,¹⁷ or very nearly so, and do not change dramatically in width or line shape as the substituent bound to the silicon atom is changed. Close inspection of Table II reveals that the ^{15}N chemical shift powder patterns and the isotropic chemical shifts indeed exhibit modest dependencies on substituent variation.

The effect of the substituent on the structure of a silatrane is perhaps most directly seen in $r_{\text{Si-N}}$. More electronegative substituents give a silatrane geometry with a smaller $r_{\text{Si-N}}$ than

(30) Bellama, J. M.; Nies, J. D.; Ben-Zvi, N. *Magn. Reson. Chem.* **1986**, *24*, 748.

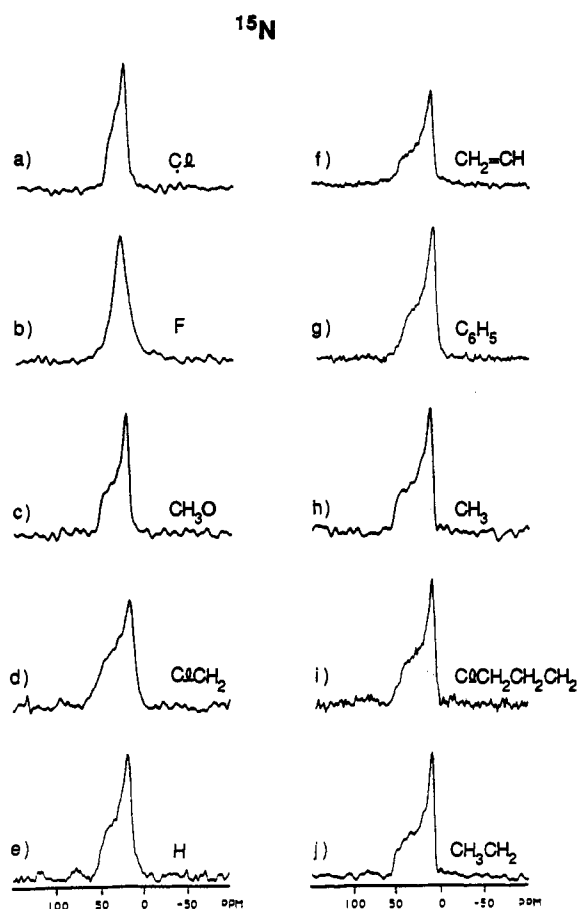
(31) Zumbulyadis, N.; Henrichs, P. M.; Young, R. H. *J. Chem. Phys.* **1981**, *75*, 1603.

(32) Harris, R. K.; Jones, J.; Ng, S. *J. Magn. Reson.* **1978**, *30*, 521.

Table II. Principal Elements of the ^{15}N Chemical Shift Powder Patterns and $r_{\text{Si-N}}$ of Selected X-Substituted Silatranes in the Solid State^a

X	δ_{\parallel}	δ_{\perp}	δ_{iso}^b	δ^c	$r_{\text{Si-N}}$ (Å) ^d	literature value for δ^e
Cl	48	21	30	32.1	2.02	
F	<i>f</i>	<i>f</i>	<i>f</i>	31.9	2.04	30.1
CH ₃ O	50	17	28	29.5	2.11 ^f	28.3
ClCH ₂ ^g	52	14	27	28.1	2.12	
H ^h	50	14	26	28.0		
CH ₂ CH ^h	53	13	26	26.3	2.15	
C ₆ H ₅ ^h	52	11	25	25.9	2.156	26.6
CH ₃	53	10	24	25.5	2.175	24.6
ClCH ₂ CH ₂ CH ₂ ^h	51	11	24	25.6	2.181	
CH ₃ CH ₂	51	7	22	23.0	2.215	

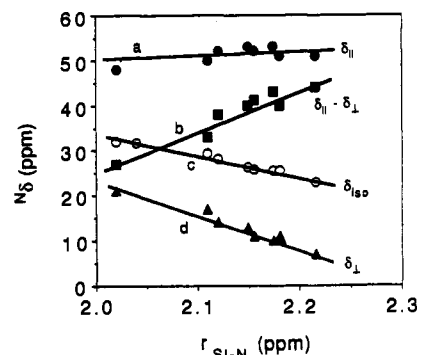
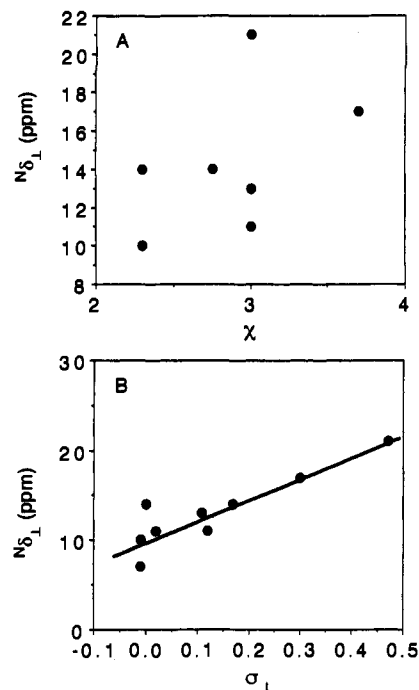
^a Chemical shift powder patterns obtained at 20.3 MHz except where noted otherwise, given in ppm relative to NH₃(l). ^b $\delta_{\text{iso}} = 1/3(\delta_{\parallel} + 2\delta_{\perp})$. ^c Isotropic chemical shift determined by CP/MAS at 20.3 MHz. ^d Data taken from ref 23. ^e Data taken from ref 33. Chemical shifts were referenced to liquid NH₃, using a value of 380.2 ppm for CH₃NO₂. ^f Chemical shift powder pattern distorted due to ^{19}F - ^{15}N heteronuclear dipole-dipole couplings. ^g Single-crystal X-ray study performed at Colorado State University. ^h Powder pattern spectra collected at 26.4 MHz.

**Figure 4.** Natural-abundance cross-polarization ^{15}N chemical shift powder patterns of X-substituted silatranes, with X indicated. Spectra were collected at 20.3 MHz for spectra a, b, c, h, and j, and at 26.4 MHz for the other spectra.

those characteristic of silatranes with less electronegative substituents. For the set of silatranes in this study, one can see from Table II that, as $r_{\text{Si-N}}$ decreases, the isotropic ^{15}N chemical shift increases, with δ_{iso} changing from 23.0 to 32.1 ppm for the ethyl and chloro derivatives, respectively. This trend has been reported previously.³³

Since δ_{iso} is nothing more than a specific combination (the mean) of the principal elements of the ^{15}N chemical shift tensor,

(33) Pestunovich, V. A.; Shterenberg, B. Z.; Lippmaa, E. T.; Myagi, M. Ya.; Alla, M. A.; Tandura, S. N.; Baryshok, V. P.; Petukhov, L. P.; Voronkov, M. G. *Dokl. Akad. Nauk SSSR* 1981, 258, 1410.

**Figure 5.** Correlation curves for some ^{15}N chemical shift parameters vs $r_{\text{Si-N}}$. (a) δ_{\parallel} , (b) $\delta_{\parallel} - \delta_{\perp}$, (c) δ_{iso} , and (d) δ_{\perp} . The solid lines are drawn for the viewers' eye.**Figure 6.** Correlation curves for the δ_{\perp} element of the ^{15}N chemical shift powder pattern of the various silatranes vs (A) χ and (B) σ_1 .

other combinations or individual elements might be expected to follow different trends. Figure 5 graphically depicts plots of various ^{15}N chemical shift parameters ($\delta_{\parallel} - \delta_{\perp}$, δ_{iso} , δ_{\parallel} and δ_{\perp}) versus $r_{\text{Si-N}}$. One recognizes a very clear correlation for $\Delta\delta$, δ_{iso} , and δ_{\perp} , while δ_{\parallel} exhibits no clear correlation. As $r_{\text{Si-N}}$ decreases, the chemical shift anisotropy, defined for an axially symmetric chemical shift powder pattern as $\Delta\delta = \delta_{\parallel} - \delta_{\perp}$ (where δ_{\parallel} is the unique element), decreases in magnitude, from 44 to 27 ppm for the ethyl and chloro derivatives, respectively. As $r_{\text{Si-N}}$ decreases, the value of δ_{\perp} approaches the value of δ_{\parallel} , with the overall result being that δ_{iso} increases. Changes in $\Delta\delta$ as well as in the isotropic chemical shift of the ^{15}N chemical shift powder patterns are due primarily to changes in the value of δ_{\perp} , which varies between 7 and 21 ppm in the samples of this study, with δ_{\parallel} being fairly constant and exhibiting no easily recognized dependence on substituent. Since the local molecular symmetry around the nitrogen atom is approximately C_{3v} , the orientation of the principal axes of the ^{15}N chemical shift powder pattern can be postulated *a priori*. On the basis of symmetry arguments,¹⁶ the δ_{\parallel} element lies along the silicon-nitrogen internuclear axis and the δ_{\perp} elements lie in a plane perpendicular to the silicon-nitrogen internuclear axis.

The variation of the δ_{\perp} elements of the ^{15}N chemical shift with respect to $r_{\text{Si-N}}$ indicates a clear dependence on the electronic-structural changes induced by the substituent. In Figure 6, it is

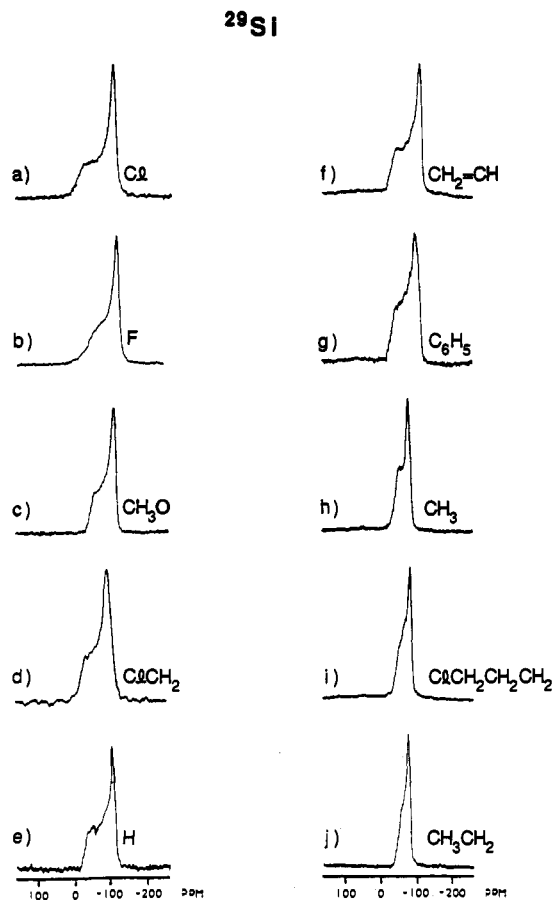


Figure 7. ²⁹Si chemical shift powder patterns collected under cross-polarization conditions at 39.8 MHz on X-substituted silatranes, with X indicated. The fluorosilatrane chemical shift powder pattern was collected under high-power ¹H and ¹⁹F decoupling conditions at 20.0 MHz.

observed that there is a rough correlation between δ_{\perp} and the Hammett-type inductive constant σ_I of the substituent but not the electronegativity χ . As σ_I increases, δ_{\perp} increases. The correlations with $r_{\text{Si-N}}$ and σ_I suggest that the substituent affects the ¹⁵N chemical shift in a twofold manner. There is an "inductive" effect in which the identity of the substituent directly affects the electronic distribution around the silicon atom, which in turn indirectly perturbs the electronic distribution around the nitrogen atom. There is also a "geometrical" effect in which the local geometry, e.g., bond lengths, internuclear distances, and bond angles, is changed, causing a redistribution of the electron density around the nitrogen atom. A natural question to ask at this point is how important the two mechanisms are in affecting the ¹⁵N chemical shift tensor. A detailed answer to this question is somewhat beyond the scope of this paper, but a qualitative answer seems relatively straightforward.

The "indirect" or geometrical-structural effect (bond angle effect), of the transannular interaction on the local nitrogen environment is rather small. Most of the shifts in atom positions induced by the transannular bond occur in the O₃Si parts of the silatrane system, as reflected in the more substantial variations in $\angle\text{OSiO}$ bond angles for a variety of silatranes.²² The average $\angle\text{CNC}$ bond angles in most silatranes are about 113°-114°. Hence, the bond angle effect of the transannular N...Si on interaction on δ is expected to be small for nitrogen. There is an indication of a very small increase in the degree of "puckering" of the C₃N fragment in silatranes with the smallest N...Si distances, e.g., for silatranes with strong inductively withdrawing X substituents. This slight puckering corresponds to a slight shift in nitrogen hybridization, away from a limit of sp² in the direction of sp³. For ¹⁵N (and ¹³C), one generally finds a trend of *increased* shielding (*decrease* in the *magnitude* of a paramagnetic shielding constant)

Table III. Principal Elements of the ²⁹Si Chemical Shift Powder Patterns in X-Substituted Silatranes^a

X	δ_{33}	δ_{22}	δ_{11}	δ_{iso}^b	δ^c	literature value for δ^d
Cl	-14	-118	-126	-86	-85.2	-86.4
F ^e	-38	-130	-138	-102	-100.4	-101.5
CH ₃ O	-50	-114	-122	-95	-95.2	
ClCH ₂	-28	-100	-117	-82	-81.9	-81.9
H	-30	-112	-116	-86	-85.8	-85.4
CH ₂ CH	-30	-106	-116	-84	-85.4	-85.3
C ₆ H ₅	-34	-100	-114	-83	-83.2	-82.9
CH ₃	-46	-80	-88	-71	-70.5	-70.8
ClCH ₂ CH ₂ CH ₂	-44	-82	-88	-71	-71.5	
CH ₃ CH ₂	-50	-78	-82	-70	-68.8	-68.7

^a Reported in ppm relative to TMS(I). ^b $\delta_{\text{iso}} = 1/3(\delta_{11} + \delta_{22} + \delta_{33})$. ^c Isotropic chemical shift measured from CP/MAS spectra. ^d Taken from ref 42 and 59. ^e The ²⁹Si chemical shift powder pattern and MAS spectrum were measured under cross-polarization conditions with ¹H and ¹⁹F decoupling at a ²⁹Si frequency of 20.0 MHz.

with increased p contribution in the hybridization³⁴ between sp² and sp³. Furthermore, Chesnut has shown in theoretical calculations³⁵ that increasing the $\angle\text{HNH}$ bond angle in ammonia (from sp³ to sp²) yields a decrease in shielding. These effects are *opposite* the trend in δ_{\perp} seen in Table II and in Figures 5 and 6 for silatranes with the smallest $r_{\text{N-Si}}$ values. Hence, we believe that the *indirect* substituent effect (i.e., due to bond angle changes) *cannot* account for the observed correlations of δ_{\perp} with $r_{\text{N-Si}}$ or σ_I .

²⁹Si Chemical Shifts. Not surprisingly, because the substituent is directly attached to silicon, the chemical shift tensor for ²⁹Si yields a more striking dependence on substituent variation than that for ¹⁵N. Although the correlations are not as "clean" as for the ¹⁵N chemical shift, the observed variation in the ²⁹Si chemical shift is much larger. The ²⁹Si chemical shift powder patterns are shown in Figure 7. The principal elements of the ²⁹Si chemical shift tensor, as well as the isotropic chemical shifts, are given in Table III. The ²⁹Si chemical shift powder patterns shown in Figure 7 correspond to chemical shift tensors that are nearly axially symmetric¹⁷ and exhibit wider variation in their anisotropies than do the ¹⁵N chemical shift powder patterns.

For ²⁹Si, $\delta_{33} - \delta_{11} = \Delta\delta$ (the anisotropy) varies from 112 to 32 ppm for the chloro and ethyl derivatives, respectively, with all of the principal elements exhibiting a dependence on the substituent. δ_{11} and δ_{22} increase by approximately 40 ppm with increasing $r_{\text{Si-N}}$, and δ_{33} decreases by approximately 20 ppm with increasing $r_{\text{Si-N}}$. The result of these trends is that δ_{iso} shows a slight dependence on $r_{\text{Si-N}}$, increasing by approximately 30 ppm as $r_{\text{Si-N}}$ increases. The ²⁹Si chemical shift powder patterns exhibit a trend that is the *reverse* of what is seen with the ¹⁵N chemical shift powder patterns; the more electron withdrawing substituents give the widest ²⁹Si chemical shift powder patterns and the least electron withdrawing substituents give the narrowest ²⁹Si chemical shift powder patterns.

As in the case of the ¹⁵N chemical shift parameters, the ²⁹Si chemical shift parameters show general trends with respect to $r_{\text{Si-N}}$. Figure 8 displays a set of chemical shift correlation curves for δ_{iso} , $\delta_{33} - \delta_{11}$, δ_{33} , and δ_{11} versus $r_{\text{Si-N}}$. The correlations are not as clear as those discussed above for the ¹⁵N data. The added complication is the presence and the local effect of the directly-attached substituent. Thus, the substituent effect on the ²⁹Si chemical shift can be viewed as having three types of origins: (1) the geometry-structure effect associated with variations in the $\angle\text{OSiO}$ bond angle; (2) the substituent effect due to variations in the N...Si transannular interaction; and (3) the direct substituent effect that would be induced even in the absence of the first two, e.g., in an analogous system without nitrogen but with the

(34) Levy, G. C.; Lichter, R. L. *Nitrogen-15 Nuclear Magnetic Resonance*; John Wiley & Sons: New York, 1979.

(35) Chesnut, D. B.; Foley, C. K. *J. Chem. Phys.* 1986, 85, 2814; 1986, 84, 852.

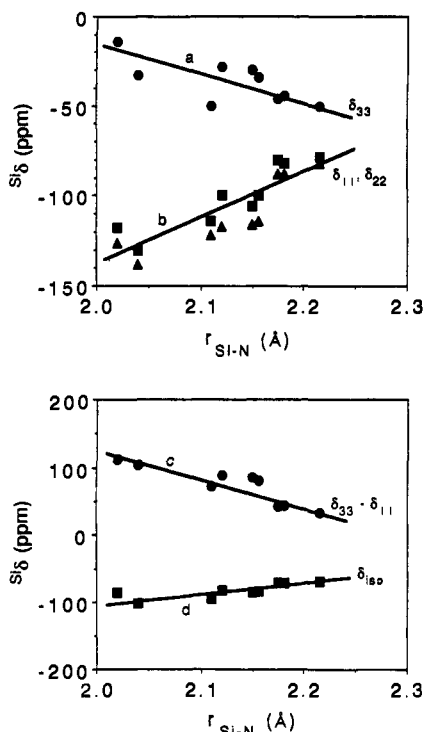


Figure 8. Correlation curves for some ^{29}Si chemical shift parameters vs $r_{\text{Si-N}}$. (a) δ_{33} , (b) δ_{11} (\blacktriangle), δ_{22} (\blacksquare), (c) $\delta_{33} - \delta_{11}$, and (d) δ_{iso} .

substituent attached to silicon. This third type of effect is, of course, absent in the ^{15}N case, so one can expect that interpretation of chemical shift data in terms of the transannular bond should be more difficult for ^{29}Si than for ^{15}N . Nevertheless, the plots in Figure 8 indicate that as $r_{\text{Si-N}}$ decreases in length, $\delta_{33} - \delta_{11}$ increases, the values of δ_{11} and δ_{22} decrease, and δ_{33} increases, with the overall result that δ_{iso} decreases. In contrast to the ^{15}N data, each of the principal elements of the ^{29}Si chemical shift tensor shows a rough dependence on $r_{\text{Si-N}}$, with the δ_{11} and δ_{22} elements more sensitive to changes in $r_{\text{Si-N}}$ than the δ_{33} element.

As in the case of the ^{15}N data, one can search for correlations between a parameter that describes the electronic properties of the substituent and the ^{29}Si chemical shift tensor elements. Figure 9 presents correlation plots of the δ_{11} element vs χ and σ_1 . The correlation plots shown in Figure 9 are not as "good" as the $r_{\text{Si-N}}$ plots shown in Figure 8 for ^{29}Si chemical shift parameters and are somewhat worse than the σ_1 plot shown in Figure 6 for the ^{15}N data. Generally, as χ and σ_1 increase the δ_{11} element of the ^{29}Si tensor decreases. The magnitude of slopes of these σ_1 and χ plots, which are greater than observed for the ^{15}N δ_{11} , may reflect simply the fact that substituent is attached directly to silicon but not to the nitrogen atom.

An analysis of the ^{29}Si chemical shift powder pattern of fluorosilatrane, including the orientation of the principal axes of the chemical shift powder pattern, has been described recently.³⁶ It was found that the axis corresponding to the δ_{33} element of the ^{29}Si chemical shift tensor is aligned parallel to the F-Si bond axis, with the axes of the δ_{22} and δ_{11} elements lying in a plane perpendicular to that bond axis. This result agrees with the expectation, based upon molecular symmetry arguments, that the most extreme ^{29}Si chemical shift tensor element has an axis aligned along the F-Si bond.

Theoretical Interpretation. At this point, a cursory examination of chemical shift theory at the independent electron MO level³⁷⁻³⁹ may be useful for exploring the effect of substituent/structure changes on the chemical shifts in silatranes. In a coordinate axis system in which the z axis is aligned along $r_{\text{Si-N}}$, the δ_{\parallel} element

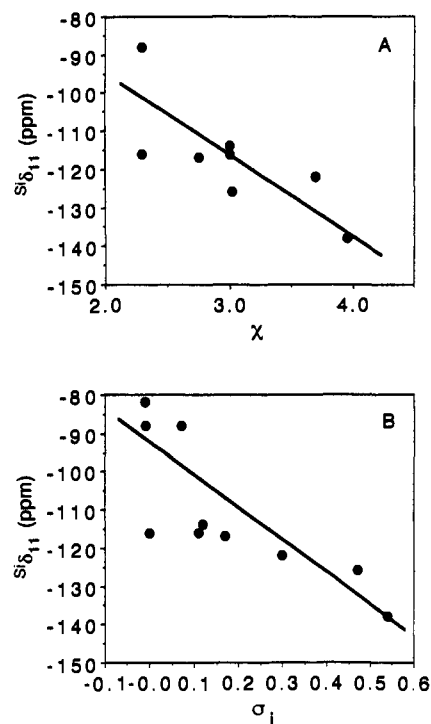


Figure 9. Correlation curves for the δ_{11} element of the ^{29}Si chemical shift powder pattern of the various silatranes vs (A) χ and (B) σ_1 .

of the ^{15}N chemical shift tensor corresponds to δ_{zz} and the δ_{\perp} elements correspond to δ_{xx} and δ_{yy} . For the ^{29}Si chemical shift tensor, the δ_{33} element corresponds to δ_{zz} and the δ_{11} and δ_{22} elements correspond to δ_{xx} and δ_{yy} .

According to popular views, the chemical shift can be split into three types of terms:

$$\delta = \delta^d + \delta^p + \sum_{C \neq A} \delta^c \quad (1)$$

where δ^d is the local diamagnetic term, δ^p is the local paramagnetic term, and the third term is a sum over all nonlocal effects.³⁷⁻⁴⁰ Pople and Karplus³⁷⁻⁴⁰ demonstrated that δ^p is primarily responsible for the variations in the chemical shift observed experimentally for ^{13}C and presumably for other nuclides of the same period. The present discussion will be based on the qualitative description of the δ^p contribution to δ .

For atoms with only s and p valence electrons, in a minimal basis set description the local contribution to the principal elements of δ^p have been described by Pople in a gauge-invariant LCAO-MO perturbation theory as follows:³⁷⁻³⁹

$$\Delta(\delta^p)_{\alpha\alpha} = (2/c^2) \langle r^{-3} \rangle_p \sum_j \sum_i^{\text{occ unocc}} (E_i - E_j)^{-1} \{ {}^A C_{\beta j} {}^A C_{\gamma i} - {}^A C_{\gamma j} - {}^A C_{\beta i} \} \sum_B \{ {}^B C_{\beta j} {}^B C_{\gamma i} - {}^B C_{\gamma j} {}^B C_{\beta i} \} - (\delta^p_{\alpha\alpha})_{\text{ref}} \quad (2)$$

where c^2 is the speed of light squared; α , β , and γ represent the x , y , and z axes; $\langle r^{-3} \rangle_p$ is the expectation value of inverse cubed radius for the p atomic orbitals on atom A; E_i and E_j are the energies of the molecular orbitals indexed by i and j ; ${}^A C_{\beta j}$ represents the zeroth-order coefficient in the j -th MO (ψ_j) of the linear combinations of atomic orbitals (LCAO) of the p atomic orbitals on atom A; and $(\delta^p_{\alpha\alpha})_{\text{ref}}$ represents the corresponding

(40) Ditchfield, R.; Ellis, P. D. *Top. Carbon-13 NMR Spectrosc.* 1974, 1, 1.

(41) Sidorkin, V. F.; Pestunovich, V. A.; Voronkov, M. G. *Dokl. Akad. Nauk SSSR* 1977, 235, 1363.

(42) Albright, T. A.; Burdett, J. K.; Whangbo, M.-H. *Orbital Interactions in Chemistry*; John Wiley: New York, 1985, p 134.

(43) Jameson, C. J.; Gutowsky, H. S. *J. Chem. Phys.* 1964, 40, 1714.

(44) Iwamiya, J. H.; Maciel, G. E. In *NATO ARW Proceedings*; Tossell, J. Ed., submitted for publication.

(36) Iwamiya, J. H.; Maciel, G. E. *J. Magn. Reson.* 1991, 92, 590.

(37) Pople, J. A. *J. Chem. Phys.* 1962, 37, 53.

(38) Pople, J. A. *J. Chem. Phys.* 1962, 37, 60.

(39) Karplus, M.; Pople, J. A. *J. Chem. Phys.* 1963, 38, 2803.

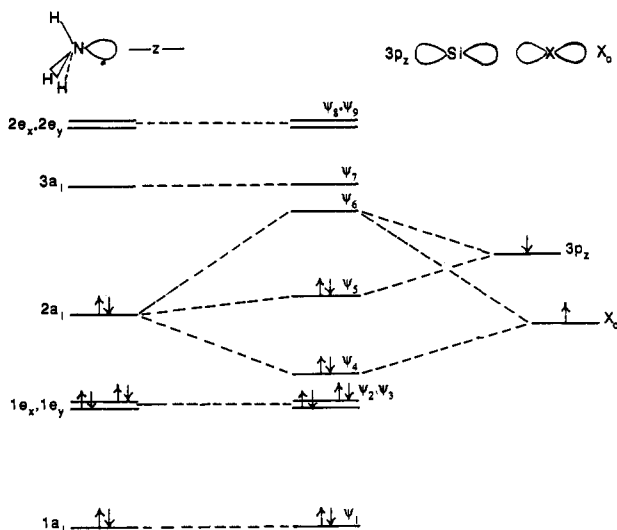


Figure 10. Simple MO diagram representing the N...Si transannular interaction, using NH_3 as a model of the nitrogen fragment of a silatrane. The MOs of NH_3 are shown on the left, the Si $3p_z$ and X orbitals on the right, and the MOs of $\text{H}_3\text{N}\cdots\text{Si}'\text{-X}$ in the middle (where Si' involves only the Si $3p_z$ orbital explicitly).

tensor element of the reference compound or site chosen as the chemical shift reference. The sums over j and i are over the occupied and unoccupied molecular orbitals, respectively, and the sum over B is over the p orbitals on all relevant (B) atoms. The absence of a negative sign in front of the right-side expression in eq 2 reflects the opposite sign conventions of chemical shift (δ) as usually defined and shielding (σ).

As silicon plays a crucial role in the silatrane structure and especially in the transannular interaction, one might expect that any useful theoretical description should include the influence of the 3d subshell of silicon. Furthermore, as the "direct" effect of the attached substituent might be expected to dominate substituent effects on ^{29}Si chemical shifts in silatranes, if one wishes to focus specifically on the transannular interaction, ^{15}N chemical shifts should be the most relevant. Since the ^{29}Si chemical shift is effected by several different influences, the rest of this discussion will focus on the effect of the transannular interaction on the ^{15}N chemical shift in silatranes. A detailed discussion of the ^{29}Si chemical shifts is beyond the scope of this paper.

The ^{15}N chemical shift will be influenced by the transannular interaction (1) "indirectly" via induced geometry changes, e.g., changes in $\angle\text{CNC}$ bond angles (which we expect to be small) and (2) "directly" by the electronic interaction between the silicon and nitrogen centers. The former effect is beyond the scope of this paper and will not here be considered further, especially in light of the considerations presented above, arguing that this effect is small. The latter effect can be discussed qualitatively in terms of eq 2.

In order to focus only on the effects of the transannular bond on the ^{15}N chemical shifts in silatranes, we adopt a simplistic MO view in which an orbital (X_0) of proper symmetry of the substituent, the $3p_z$ orbital of silicon, the lone pair on nitrogen, and the remainder of an NH_3 MOs are considered explicitly and the rest of the silatrane bonding network is viewed as a framework that is essentially unperturbed by the N...Si bond. We construct a simplified model of the local nitrogen structure and the influence of the substituent-bound silicon atom by an idealized MO diagram based on the previously proposed idea of a three-center "hypervalent" N...Si—X bond.⁴¹ This model, shown in Figure 10, reflects the prevailing view of bonding in silatranes, recognizing the fact that $\angle\text{OSiO}$ angles in silatranes are close to 120° ; this corresponds to the use of sp^2 silicon atomic orbitals in the Si—O bonds and the consequent availability of the $3p_z$ orbital of silicon for the transannular bond.

The MO picture in Figure 10 shows a simple MO diagram of NH_3 on the left,⁴² the $3p_z$ silicon orbital and a suitable X orbital on the right, and a simple silatrane MO diagram constructed as a combination of the "lone-pair" nitrogen orbital ($2a_1$), the silicon $3p_z$, and X_0 of the substituent. Using NH_3 as the nitrogen fragment in this model does not include the 2s and 2p orbitals of the bound carbons of a silatrane. Such orbitals would, of course, have to be included in the formal application of eq 2 to the silatrane case, but we will consider those aspects of the problem to be largely unchanged by the N...Si interaction. This simplified MO diagram of Figure 10 is used in this qualitative attempt in order to focus explicitly on the effect of the transannular interaction on ^{15}N .

The simple MO model shown in Figure 10 incorporates ideas embodied in published MO descriptions of silatranes.^{22,41} However, the scheme in Figure 10 is not set up to explore consequences on energies, bond angles, or bond lengths or even the existence of a transannular bond. The MO scheme of Figure 10 *assumes* the existence of a transannular bond and is designed for exploring the influence of that interaction on the ^{15}N chemical shift.

For the simplified silatrane nitrogen model of Figure 10, there are 10 electrons, so the lowest five MOs are occupied. The only (partially) occupied p orbital of silicon is $3p_z$, the extent of occupation embodied in the appropriate coefficient in ψ_5 .

There are some general qualitative statements that can be made about the effect of the N...Si transannular interaction on the ^{15}N chemical shift. One should expect that the involvement of a N...Si interaction in the local electronic structure of nitrogen should, other things being equal, increase the *magnitude* of σ^p (or the algebraic value of δ^p) by introducing nonzero coefficients for the *same* MO for N and Si into the two terms in brackets in eq 2, yielding nonzero contributions to ^{15}N . Hence, it is not surprising that the ^{15}N shielding (especially $^{15}\text{N}_{\perp}$) is smaller (^{15}N δ is larger) for silatranes with the strongest N...Si interactions (smallest $r_{\text{Si-N}}$; see Table II). Because of the z-symmetry of the N...Si transannular interaction, as embodied in the MO diagram of Figure 10, the prediction of an equation of the type of eq 2 is that substituent-induced variations in the transannular bond should have no effect on $^{15}\text{N}_{\parallel}$. This is consistent with the nearly invariant value of $^{15}\text{N}_{\parallel}$ for the silatranes represented in this study (Table II). For that reason, we will limit our further theoretical discussion in this paper to $^{15}\text{N}_{\perp}$.

A second statement is based on the fact that the factor $\langle r^{-3} \rangle_p$ in eq 2 is influenced by any effect that changes the "size" of a 2p orbital on nitrogen. A substituent that withdraws electron density inductively from nitrogen would increase the "effective nuclear charge" on nitrogen,⁴³ decreasing the size of a 2p orbital and hence increasing $\langle r^{-3} \rangle_p$ and the magnitude of $^{15}\text{N}_{\perp}$. This prediction is consistent with the experimental trend seen in Table II and Figure 6, i.e., that increasing the σ_1 value of the substituents brings about an increase in $^{15}\text{N}_{\perp}$ (an increase in the magnitude of the paramagnetic shielding term). This focus on $\langle r^{-3} \rangle_p$ effects also makes it possible to rationalize the rough, monotonic correlation (not shown here) between the "perpendicular" ^{15}N and ^{29}Si chemical shift elements, $^{15}\text{N}_{\perp}$ and $1/2(\text{Si}\delta_{11} + \text{Si}\delta_{22})$; one of these parameters increases and the other decreases as $r_{\text{Si-N}}$ varies with substituent. If an inductive effect that alters the local atomic charge on nitrogen does so at least partly at the expense of the local electronic charge of silicon (e.g., an alternating inductive polarization effect), then the effects on $\langle r^{-3} \rangle_p$ for silicon and nitrogen should be opposite in sign. This should lead to opposite effects on $^{15}\text{N}_{\sigma_p}$ and $^{29}\text{Si}_{\sigma_p}$ or on $^{15}\text{N}_{\delta_p}$ and $^{29}\text{Si}_{\delta_p}$, as observed experimentally.

The orbital energy levels shown pictorially in Figure 10 correspond to the previously suggested case of a three-center hypervalent N...Si—X bond.⁴¹ According to that qualitative MO treatment, an X_0 orbital with an effective electronegativity larger than that of the silicon $3p_z$ orbital ($\alpha_{X_0} \ll |\alpha_{3p_z}|$, where α is a Coulomb integral) leads to an increase in the bond energy

(strength) of the N...Si interaction and hence a smaller N...Si internuclear distance. Such an effect would redistribute nitrogen lone-pair character among the ψ_4 , ψ_5 , and ψ_6 MOs, two of which are occupied. This redistribution of nitrogen lone-pair character among occupied and unoccupied orbitals (relative to simply one occupied and one unoccupied orbital corresponding to the nitrogen lone pair that is not involved in a N...Si interaction) can be expected to increase the magnitude of the coefficient expressions (in brackets) in eq 2. Coefficients for both occupied (j) and unoccupied (i) MOs and for both $2a_1$ and $3p$, orbitals must be nonzero in order for the product of the coefficient expressions in brackets to be nonzero. This would also lead to an increase in $|\delta_{\perp}^p|$ and an increase in δ_{\perp} as the transannular interaction is enhanced. This is the trend found experimentally for increasing σ_1 .

Without actually performing high-quality MO calculations, it would be difficult to predict quantitatively the effects of substituent variation on the relevant energy differences, $E_i - E_j$, in eq 2. Furthermore, at a higher level of MO calculation there are more sophisticated and more accurate computational theories of chemical shifts than what is represented in eqs 1 and 2. *Ab initio* perturbed Hartree-Fock calculations on small systems designed to model silatranes have been carried out with mixed success.⁴⁴ Nevertheless, it is worth noting that data from electronic spectroscopy²² indicates that the substitution of silatrane by an electron withdrawing group (X) leads to a shift to larger wavelength in the transitions observed. To the extent that such transitions correspond, even qualitatively, to the relevant "excitations" of Figure 10 in the Pople formalism, this kind of shift would lead to an increase in the magnitude of σ^p and hence a shift to lower shielding.

Hence, all of the qualitative considerations based on eq 2 lead to the same general conclusions regarding ^{15}N chemical shifts in silatranes: (1) δ_{\perp} should be much more sensitive to variations in the transannular interaction induced by effects of Si-attached substituents and (2) inductively withdrawing substituents cause substantial increases in the magnitude of δ_{\perp}^p (increases in δ_{\perp}).

Summary

It is apparent that among the chemical shift parameters that can be measured in the solid state for the Si-substituted silatranes, those of ^{15}N and ^{29}Si provide the most direct and easily obtained information and are most sensitive to substituent-induced changes in the molecular/electronic structure of silatranes. The ^{15}N and ^{29}Si chemical shift powder patterns, especially the former, are promising for providing insight into the silicon-nitrogen transannular interaction. The value of ${}^{\text{N}}\delta_{\perp}$ correlates well with $r_{\text{Si-N}}$ and with σ_1 and appears to be a *direct measure of the transannular interaction*.

For ^{15}N , the parameter δ_{\perp} , which from local symmetry considerations is along the Si—N internuclear axis, apparently does not vary substantially with changes in X (or $r_{\text{Si-N}}$), in agreement with the predictions of a simple MO theory. The ^{15}N chemical shift tensor monitors variations in nitrogen's local electronic distribution that correlate with variation of the substituent on the silicon atom, monitoring the transannular interaction directly.

For the ^{29}Si chemical shift powder pattern, correlations are found between δ_{11} , δ_{22} , δ_{33} , and $r_{\text{Si-N}}$. These correlations are not as simple to interpret as for the ^{15}N results because the ^{29}Si chemical shift tensor is strongly affected by the directly attached substituent as well as by the silicon-nitrogen transannular interaction.

Acknowledgment. The authors gratefully acknowledge support of this research by NSF Grant No. CHE-9021003. J.H.I. acknowledges the financial support of a N.A.S.A. Training grant. The authors also thank Professor Leo Sommer of the University of California, Davis, for supplying some of the silatranes used in this study and Professor Oren P. Anderson (C.S.U.) for the X-ray structure determination of methoxysilatrane.